ESC European Society of Cardiology

Cardiovascular Research (2023) **119**, 1553–1567
https://doi.org/10.1093/cvr/cvad040

VEGF-B hypertrophy predisposes to transition from diastolic to systolic heart failure in hypertensive rats

Anne-Maj Samuelsson [1,2]*, Theda Ulrike Patricia Bartolomaeus [3,4,5,6], Harithaa Anandakumar[3,4,5,6], Irene Thowsen[1], Elham Nikpey[1], Jianhua Han[1,2], Lajos Marko[3,4,5,6], Kenneth Finne [7], Olav Tenstad [1], Johannes Eckstein [8], Nikolaus Berndt [9,10], Titus Kühne [9,10], Sarah Kedziora[3,4,5,6], Ibrahim Sultan[11], Trude Skogstrand[1], Tine V. Karlsen [1], Harri Nurmi [11], Sofia K. Forslund [3,4,5,6], Entela Bollano [12], Kari Alitalo [11], Dominik N. Muller [3,4,5,6], and Helge Wiig [1]

[1]Department of Biomedicine, University of Bergen, Jonas Leis vei 91, 5020 Bergen, Norway; [2]Department of Medicine, Haukeland University Hospital, Jonas Leis vei 65, 5021 Bergen, Norway; [3]Experimental and Clinical Research Center (ECRC), a joint cooperation between Charité Universitätsmedizin Berlin and Max-Delbrück-Center for Molecular Medicine, Lindenberger Weg 80, 13125 Berlin, Germany; [4]Max-Delbrück-Center for Molecular Medicine in the Helmholtz Association (MDC), Robert-Rössle-Straße 10, 13125 Berlin, Germany; [5]Charité Universitätsmedizin Berlin, Corporate Member of Freie Universität Berlin, Humboldt Universität zu Berlin, and Berlin Institute of Health, Charité platz 1, 10117 Berlin, Germany; [6]DZHK (German Centre for Cardiovascular Research), partner site Berlin, Potsdamer Straße 58, 10785 Berlin, Germany; [7]Department of Clinical Medicine, University of Bergen, Jonas Lies vei 87, 5021 Bergen, Norway; [8]Charité Universitätsmedizin Berlin, Corporate Member of Freie Universität Berlin and Humboldt-Universität zu Berlin, Institute of Biochemistry, Charité-University Medicine, Augustenburger Platz 1, 13353 Berlin, Germany; [9]Deutsches Herzzentrum der Charité (DHZC), Institute of Computer-assisted Cardiovascular Medicine, Augustenburger Platz 1, 13353 Berlin, Germany; [10]Charité-Universitätsmedizin Berlin, Corporate Member of Freie Universität Berlin and Humboldt-Universität zu Berlin, Charite Platz 1, 10117 Berlin, Germany; [11]Wihuri Research Institute and Translational Cancer Medicine Program, Biomedicum Helsinki, University of Helsinki, Haartmaninkatu 8, 00290 Helsinki, Finland; and [12]Department of Cardiology, Sahlgrenska University Hospital, Blå stråket 5, 413 45 Göteborg, Sweden

Received 31 January 2022; revised 4 October 2022; accepted 10 January 2023; online publish-ahead-of-print 23 March 2023

Aims

Cardiac energy metabolism is centrally involved in heart failure (HF), although the direction of the metabolic alterations is complex and likely dependent on the particular stage of HF progression. Vascular endothelial growth factor B (VEGF-B) has been shown to modulate metabolic processes and to induce physiological cardiac hypertrophy; thus, it could be cardioprotective in the failing myocardium. This study investigates the role of VEGF-B in cardiac proteomic and metabolic adaptation in HF during aldosterone and high-salt hypertensive challenges.

Methods and results

Male rats overexpressing the cardiac-specific VEGF-B transgene (VEGF-B TG) were treated for 3 or 6 weeks with deoxycorticosterone-acetate combined with a high-salt (HS) diet (DOCA + HS) to induce hypertension and cardiac damage. Extensive longitudinal echocardiographic studies of HF progression were conducted, starting at baseline. Sham-treated rats served as controls. To evaluate the metabolic alterations associated with HF, cardiac proteomics by mass spectrometry was performed. Hypertrophic non-treated VEGF-B TG hearts demonstrated high oxygen and adenosine triphosphate (ATP) demand with early onset of diastolic dysfunction. Administration of DOCA + HS to VEGF-B TG rats for 6 weeks amplified the progression from cardiac hypertrophy to HF, with a drastic drop in heart ATP concentration. Dobutamine stress echocardiographic analyses uncovered a significantly impaired systolic reserve. Mechanistically, the hallmark of the failing TG heart was an abnormal energy metabolism with decreased mitochondrial ATP, preceding the attenuated cardiac performance and leading to systolic HF.

Conclusions

This study shows that the VEGF-B TG accelerates metabolic maladaptation which precedes structural cardiomyopathy in experimental hypertension and ultimately leads to systolic HF.

* Corresponding author. Tel: +47 5558 6387, fax: +47 5558 6360, E-mails: annemaj@stanford.edu; annemaj.samuelsson8@gmail.com; anne-maj.samuelsson@uib.no

Graphical Abstract

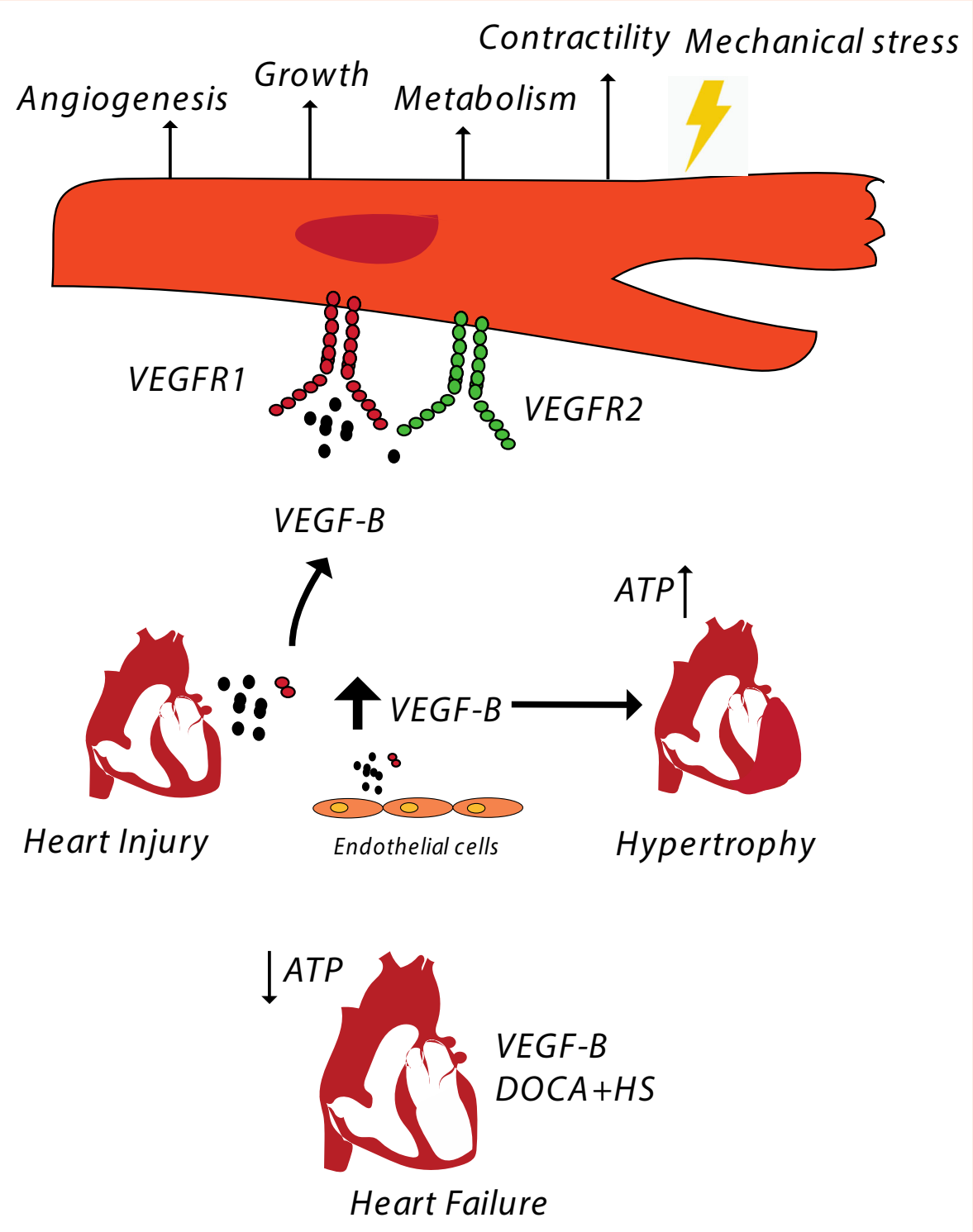

Keywords VEGF-B • Heart failure • Cardiac hypertrophy • Metabolism • Salt • Aldosterone

1. Introduction

Cardiac hypertrophy is a leading cause of chronic HF (CHF), which in turn is one of the most common fatal long-term cardiac complications. Today, there are approximately 26 million individuals that have been diagnosed to have CHF. This incidence is predicted to rise to a staggering 77 million in 2040 because of progressive population aging globally.[1] Despite the

accuracy of today's biomarkers for diagnosing HF, the disease is progressive, and no effective treatment exists. Both animal models of HF and human HF disease show first hypertrophic impairment of cardiac function in association with derangement in cardiac energy metabolism and mitochondrial function, which contribute to the pathological remodelling which leads to CHF.[2] The capacity of cardiac mitochondria to generate adenosine triphosphate (ATP) is further compromised during the development of HF.[3] The regulatory events and their timing involved in the metabolic reprogramming of the hypertrophic and failing heart remain largely unknown. To date, studies have focused largely on mechanisms of candidate gene regulation in severe, late-stage disease, and less on the transition from HF with preserved ejection fraction (HFpEF) to HF with reduced ejection fraction (HFrEF).[4] Accordingly, such studies may not offer useful insights into the primary mechanisms and trajectories that drive early alterations of energy metabolism in pathological cardiac remodelling. Characterization of the disturbed fuel and energy metabolism and mechanism of its upstream regulation in the early stages of HF are important first steps towards the identification of new therapeutic targets for the treatment of early-stage HF.[5]

Vascular endothelial growth factor (VEGF)-B is structurally the closest homologue of VEGF-A, but functionally very different from it. Unlike VEGF-A gene deletion, VEGF-B deletion does not affect angiogenesis during mouse embryonic development, or wound healing or pathological processes in adult mice.[6] Interestingly, however, VEGF-B gene transfer stimulates blood vessel growth in the heart and adipose tissues.[7] Coronary vessel growth induced by VEGF-B leads to cardiac hypertrophy without progression to cardiomyopathy, and VEGF-B gene transfer to adult heart has been shown to protect the heart from ischaemic damage.[8] Bioinformatic analysis has indicated that VEGF-B expression correlates with the expression of nuclear-encoded mitochondrial genes across a large variety of physiological conditions in mice, suggesting that it could affect metabolic processes during pathological cardiac remodelling.[9] In order to find out if VEGF-B can protect the heart from pressure overload induced stress, we investigated the consequences of increased VEGF-B in an established salt-sensitive hypertension model in rats. In this model, an excess of mineralocorticoid caused by chronic administration of deoxycorticosterone acetate together with high salt (HS) (DOCA + HS) induces cardiac hypertrophy and cardiac fibrosis.[10]

Cardiac contractility is dependent on continuous production of ATP, which is generated by oxidative phosphorylation (OXPHOS) in mitochondria. Thus, it is not surprising that mitochondrial defects are associated with heart injury induced by myocardial infarction (MI). Indeed, reduced ATP generation resulting from inadequate mitochondrial OXPHOS is a fundamental mechanism in impaired cardiac contractility.[11] The hallmark of inadequate OXPHOS includes oxidative stress and utilization of alternative mechanisms of energy production, as shown by the metabolomic alterations in the heart in numerous models of cardiac injury, including MI/ischaemia and HF.[12] To date, however, no proteomics analyses have been published in VEGF-B transgenic (TG)-mediated hypertrophy during increased preload. Also, the extent to which VEGF-B affects stress-induced energy production and metabolism in the heart is unknown.

VEGF-B expression was reported to be declined in patients with HF, where circulating VEGF-B levels are inversely correlated with ongoing left ventricular remodelling.[13,14] We therefore considered that myocardial delivery of VEGF-B could be therapeutic in cardiac remodelling during stress induced hypertrophy, when VEGF-B reverts transiently metabolic function to a hypermetabolic state. We further considered that such effect of VEGF-B might chronically alleviate energy exhaustion including decrease of ATP, in progression to HF. In agreement with our hypothesis, ATP increase induced by VEGF-B overexpression in the hypertrophic heart prevented the decrease of cardiac systolic function. Surprisingly, the protective effect of the cardiac function was observed in early-stage remodelling, while chronic VEGF-B overexpression appeared to drive the transition of diastolic (HFpEF) to systolic HF (HFrEF). These findings suggest that the subsequent decline in cardiac function was caused by a defective myocardial energy metabolism, indicating that the metabolic shift promoted by VEGF-B gene delivery is beneficial during acute cardiac remodelling but could become detrimental in the long term.

2. Methods

The authors declare that all supporting data and analytical methods are available within the article and its Supplementary material online, *Method*. All materials used for this study are listed with their respective sources in *Supplementary material online*, Table *S1*. The data, analytical methods, and study materials that support the findings of this study are available from the corresponding authors on reasonable request. All animals received human care according to the standards of Annex III of the directive 2010/63/EU of the European Parliament on the protection of animals used for scientific purposes. All the experiments were carried out in accordance with regulations of the Norwegian State Commission for Laboratory Animals, and with approval from the AAALAC International accredited Animal Care and Use Program at University of Bergen (license no. FOTS ID 10508). The VEGF-B TG (αMHC-VEGF-B) rats of outbred HsdBrl:WH Wistar background have been previously described.[15] A total of 50 VEGF-B TG and WT male rats were group-housed under controlled environment with a temperature of 22°C and a 12-h light/dark cycle and fed control diet ad libitum (RM1#801151, Special Diet Services, UK) . For all procedures, rats were anaesthetized with isoflurane in oxygen (4% induction, 1.5% maintenance, flow rate, 1–2 L/min) and injected with one dose of pre- and post-operative analgesia (Buprenorphine, 0.1 mg/kg, s.c.). After baseline recordings (telemetry and echocardiography) rats were implanted with DOCA (2 × 150 mg/pellet, Innovative Research of America, Sarasota, FL, USA) s.c. and assigned to 1% saline (HS) in the drinking water for six consecutive weeks. Transthoracic echocardiography was performed in all WT and TG rats (total of 50) before and after DOCA-HS ($n = 32$) and sham operation ($n = 18$), with a sub-group of 12 rats (6 WT and 6 TG) assigned to the weekly continuous echocardiographic study. Tissue harvest was conducted after echocardiographic measurements at baseline ($n = 18$), Week 3 ($n = 16$), and Week 6 ($n = 16$) DOCA-HS. Additionally, acute LV volumetric and functional changes were assessed after an intraperitoneal bolus injection of the β-receptor agonist dobutamine (1.0 mg/kg bw) (see Supplementary materials online). Water intake and urine volume were measured before and after DOCA-HS challenge, with no sign of dehydration in either WT and VEGF-B TG rats (data not shown). At the end of the study, all rats were euthanized while fully anesthetized by inhalation of isoflurane (5%) until respiration ceased, followed by bilateral thoracotomy for cardiac blood collection. The outline of our study is given in Supplementary material online, *Figure S1A*.

3. Results

3.1 VEGF-B TG rats develop cardiac hypertrophy and early signs of diastolic dysfunction

The overall objective of this study was to test whether cardiac VEGF-B overexpression (VEGF-B TG rats) can improve cardiac pathology and metabolic dysfunction in salt sensitive hypertension. We used rats with increased human VEGF-B expression in the heart under the control of rat αMHC gene promoter to determine baseline and stress-induced longitudinal heart characteristics, as shown in *Figure 1A*. At the baseline, as expected on the basis of previous publications,[16] 8-month-old VEGF-B TG male rats exhibit increased VEGF-B levels in the heart and serum (see Supplementary material online, *Figure S1I and J*) with a concentric hypertrophic phenotype (heart weight-to-tibia ratio +39% and relative wall thickness +59% compared to WT), with larger cardiomyocytes and increased metabolic ATP demand (*Figure 1B–F and L*). Consistent with previous findings[7,8] the TG rats demonstrated myocardial hypervascularization, with proportionally larger arteries, particularly near the endocardium (*Figure 1G and H*). This hypervascularization was accompanied by an excess of water in the heart

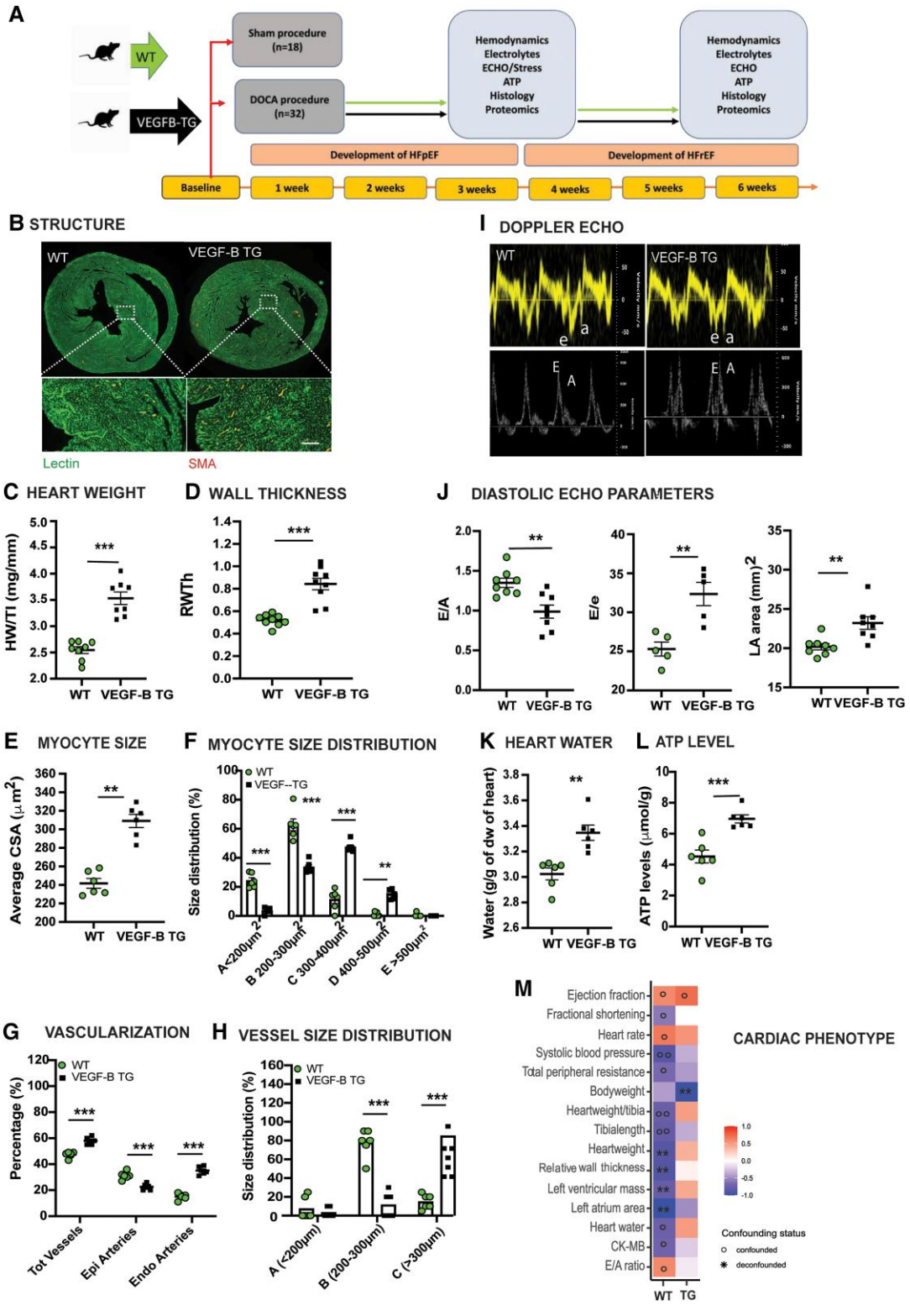

Figure 1 Cardiomyocyte-specific VEGF-B induces cardiac hypertrophy and diastolic dysfunction at baseline. (*A*) Longitudinal DOCA + HS protocol of the transition phase between diastolic HF and systolic HF in WT and VEGF-B TG rats. (*B*) Overall scan of the cardiac section (Lycopersicon Esculentum Lectin) showing thickening of LV wall in TG rats with close-up images of septal region showing increased α smooth muscle actin (αSMA) expression. Scale bar 50μm. (*C*) Heart weight normalized to tibial length (HW/TI) and (*D*) heart relative wall thickness (RWTh) in the VEGF-B TG and the WT rats ($n = 8$). Data are depicted as dot plots with mean ± SE and were analyzed by unpaired, two-tailed *t*-test. Quantitative data for (*E*) myocyte cross-sectional area (CSA) and (*F*) myocyte size distribution, assessed by H&E staining (original magnification × 20) in VEGF-B TG and WT rats ($n = 6$). (*G*) Heart vascularization and (*H*) vessel diameter assessed by CD31 antibody in VEGF-B TG and WT rats ($n = 5$–8). Fixed quantity of vessels in total heart and in the different regions of the heart

(continued)

Figure 1 Continued
(epicardium and endocardium) of the cardiac tissue of VEGF-B TG and WT rats. Significance was analyzed by unpaired, two-tailed *t*-test. (*I*) Representative Doppler Echocardiographic tracings of TG and WT hearts demonstrating A- and E-peak and tissue Doppler e-peak. (*J*) Diastolic heart function: Levels of E/A, E/e, and left atrium area (LA area) in VEGF-B TG and WT rats ($n = 5–8$). Data are depicted as dot plots with mean ± SE and analyzed by unpaired, two-tailed *t*-test. (*K*) Heart water content using gravimetry measurements of TG and WT hearts ($n = 6$). (*L*) ATP concentration (µmol/g) in LV tissue in WT and VEGF-B TG rats. ***$P < 0.001$, **$P < 0.01$, *$P < 0.05$ vs. WT; unpaired, two-tailed *t*-test. (*M*) MetadeconfoundR analysis for univariate biomarkers controlling for potential confounders under parallel post hoc testing using nested linear model comparisons: clinical impact of genotype (WT vs. VEGF-B TG). Heatmap shows all clinical features significantly [MWU (for categorical factors) and Spearman (for continuous features) *FDR < 0.1, **FDR < 0.01, ***FDR < 0.001] different in different between genotypes. Heatmap cells show effect size (Cliff's Delta for categorical factors, Spearman's Rho for continuous features). Features with at least one clear confounder shown with grey circle markers, others with black asterisks. Systolic BP, creatine kinase MB (CK-MB), TPR, tibial length (TI), HR, LVMass, relative wall thickness (RWTh), left atrium (LA) area, FS, EF, and heart water. Taken together, these findings suggested that cardiomyocyte-specific VEGF-B overexpression induced cardiac hypertrophy and revascularization. The TG rats also developed a degree of diastolic dysfunction.

(+11%, *Figure 1K*). Gradual fluid accumulation has been associated with diastolic dysfunction.[17] Accordingly, detailed doppler echocardiography analysis demonstrated mild diastolic dysfunction in TG rats with altered LV filling in diastole (increased A velocity), restrictive relaxation E-wave and E/A ratio (*Figure 1I* and *J*). The ratio of E-wave to mitral annular e velocity (E/e), a reliable predictor of LV end-diastolic pressure (*Figure 1J*) was significantly higher in the TG rats, suggesting greater LV filling pressures and prolonged IVRT indicated poor myocardial relaxation. All these changes could be related to the significantly elevated night blood pressure (BP) afterload (>5 mmHg, Supplementary material online, *Figure S1A and B*) and the LV hypertrophy (*Figure 1C*). The diastolic dysfunction was further supported by altered myocardial performance index (tei), which revealed a significant increase in diastolic stiffness coefficient in the TG rats (see Supplementary material online, *Figure S1C–E*). Myocardial relaxation involves changes in processes such as calcium handling, as well as myocardial energetics and intrinsic physical properties of the LV. VEGF-B TG rats demonstrated increased heart Ca^{2+} (see Supplementary material online, *Figure S1G*) and ATP content (*Figure 1L*), which all are increasingly recognized in human HF progression.[18] The Na+ and K+ levels in the hearts of VEGF-B TG and WT rats were similar (see Supplementary material online, *Figure S1H and I*). Some clinical features that were assessed in the WT and TG rats are shown in the heatmap indicating the statistical significance and the effect size (see Supplementary material online, *Figure S1F, I, and M*). The WT rats were significantly heavier (TG, 345 ± 5 g vs. WT, 374 ± 7 g, $P < 0.01$), and the TG rats had significantly higher hemodynamic pressure [BP, total peripheral resistance (TPR)], heart weight and wall thickness than the WT rats. Taken together, at the baseline, the VEGF-B TG rats had concentric LV hypertrophy with mild diastolic dysfunction and chamber stiffness. This suggested that they might be more vulnerable to a 'second hit', such as hypertension.

3.2 Mineralocorticoid signalling induces impaired systolic reserve in VEGF-B TG rats

Aldosterone and salt are both known to increase cardiovascular risk in humans.[19] We used the DOCA + HS treatment as such a 'second hit' to provoke cardiac damage analogous to what can be expected to happen in at-risk human patients. As expected, chronic DOCA + HS (3 and 6 weeks) challenge led to a sustained increase in afterload (BP and TPR traces presented in Supplementary material online, *Figure S2A and B*). The TG rats demonstrated cardiac hypertrophy prior to challenge which plateaued to WT levels after 3 weeks DOCA-HS challenge, with significantly thicker LV walls in TG than WT hearts (*Figure 2A–D*). Systolic function, measured as fractional shortening (FS), ejection fraction (EF), stroke volume (SV), and cardiac output (CO), was preserved at 3 weeks (*Figure 2E–H*). Diastolic parameters E/A (<1.5), E/e, LA area, and the tei index (MPI > 1.2, *Figure 2I* and *J*; Supplementary material online, *Figure S2C and D*) showed impaired relaxation in both genotypes as the intervention progressed, with increased interstitial fibrosis and collagen, more prominently in the TG rats (see Supplementary material online, *Figure S2E–H*).

After 6 weeks of DOCA + HS treatment, the VEGF-B TG rats displayed signs of dilated cardiomyopathy (DCM) (*Figure 2A–C*) with thinning of the LV wall (*Figure 2D*) and dilation of LV internal diameters when compared with WT rats (*Figure 2C*). This dilatory phenotype was associated with impaired systolic function in the TG vs. WT rats, as evidenced by a reduced FS (45 ± 1% vs. 55 ± 2%, $P < 0.05$), EF (48 ± 3% vs. 63 ± 1, $P < 0.001$), and CO (55.5 ± 1.6 mL/min vs. 76.3 ± 1.7 mL/min, $P < 0.001$) (*Figure 2E, F, and H*). Furthermore, mitral valve Doppler imaging displayed increased E/A and E/e ratios in the treated TG rats, indicative of impaired LV relaxation and diastolic dysfunction (*Figure 2I and J*). In line with the macroscopic changes in the VEGF-B TG hearts, they had thinner cardiomyocytes and elongated sarcomeres in histological comparison with WT rats (see Supplementary material online, *Figure S3A and B*). Furthermore, the VEGF-B TG rats demonstrated significantly higher water content in the lungs and hearts (see Supplementary material online, *Figure S3C and D*).

Cardiac response to inotropic dobutamine stimulation is proved to be a sensitive tool to identify early signs of systolic dysfunction in rats and to foresee HF progression.[20] Although the resting systolic function was similar in the WT and TG rats after 3 weeks of DOCA + HS treatment, we found that upon dobutamine challenge, the VEGF-B TG rats had impaired systolic reserve to stress, with reduced systolic performance vs. WT rats [ΔLVESD (left ventricle end systolic diameter), −0.84 vs. −1.47 mm, $P = 0.008$, *Figure 2N*], and impaired cardiac reserve (ΔFS, 7 vs. 18%, $P = 0.002$, and ΔCO 6.6 vs. 18.3 mL/min $P = 0.004$, *Figure 2Q*; Supplementary material online *Figure S3I*) and chronotropic reserve (ΔEF, 12 vs. 17% $P < 0.01$, Supplementary material online, *Figure S3G*). Similar characteristics have been reported in chronically failing human hearts during an early stage of HF, without any abnormalities in the resting systolic function.[21] Two VEGF-B TG rats died after dobutamine challenge, further strengthening previous result that the hypertrophic VEGF-B TG hearts are more susceptible to cardiac arrythmias.[22] Thus, we did not proceed with stress echocardiography at Week 6. Longitudinal stress echocardiography from baseline to Week 3 is presented in Supplementary material online, *Figure S3E*. Some of the systolic parameters diverged already at Week 2, with loss of responsiveness in the TG rats (see Supplementary material online, *Figure S3F–J*). In all TG rats, increased afterload for 3 weeks led to diastolic dysfunction and cardiac fibrosis. Thus, dobutamine stress echocardiography, uncovered an impaired systolic reserve in the VEGF-B TG rats that preceded systolic dysfunction, suggesting a transition to a more decompensatory HF phenotype.

3.3 DOCA—salt hypertension promotes HF transition from preserved to reduced EF in hypertrophic VEGF-B hearts

LV remodelling and progressive dysfunction are processes that culminate into an end-stage HF. The stages that precede this severe condition are still poorly known, thus representing an important target for research. Our longitudinal phenotyping offered a unique opportunity to study cardiac functional parameters on a weekly basis and thus to evaluate the transition from diastolic HF to systolic HF. The LV EF trajectories diverged considerably between the VEGF-B TG vs. WT rats (*Figure 3A*). During Weeks 1–3 of DOCA + HS challenge, the TG rats had an upward EF trend, but starting at Week 4 they demonstrated a gradual decline in EF. This was associated

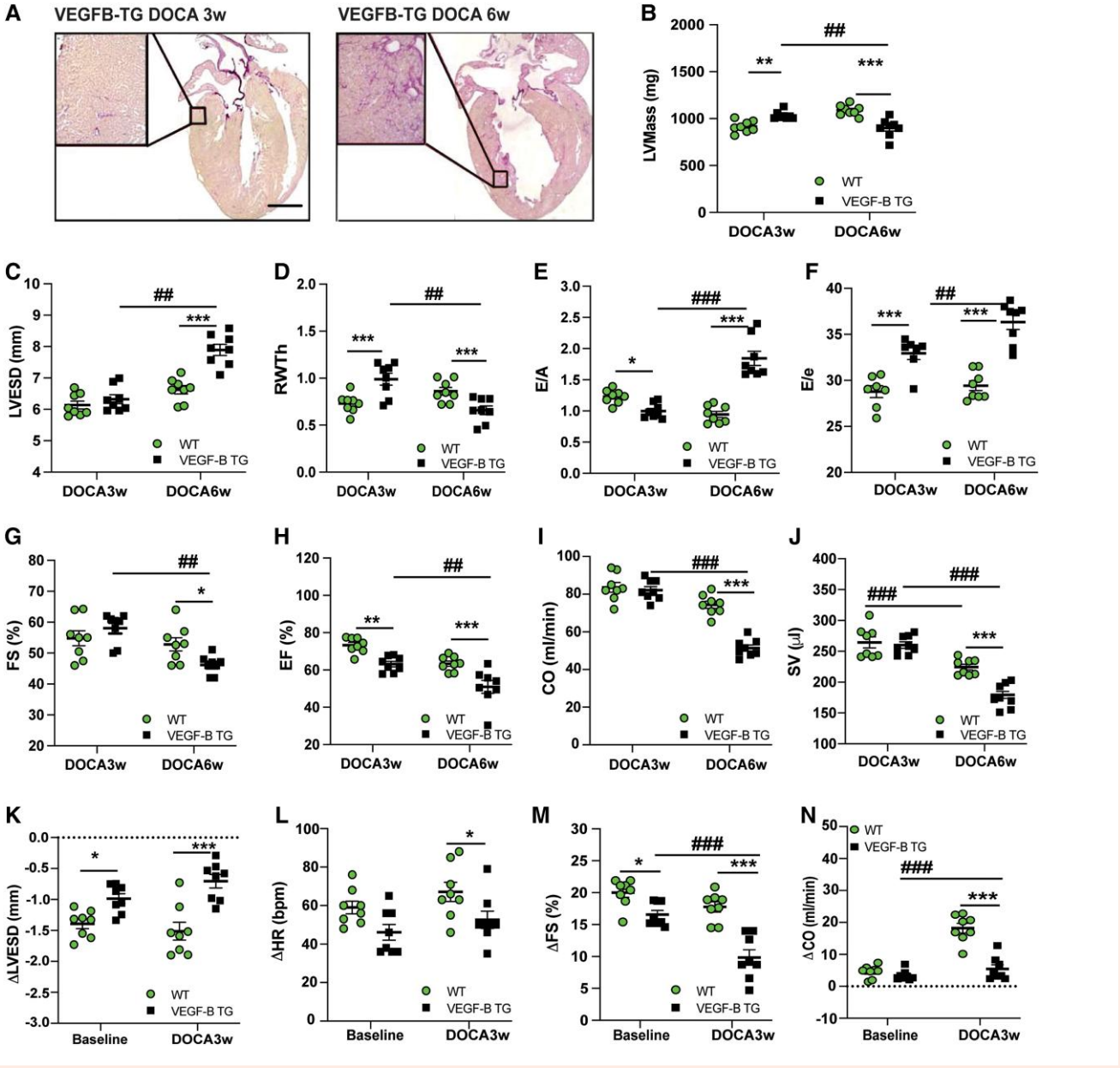

Figure 2 Increased afterload (DOCA + HS) leads to progressive diastolic dysfunction and impaired cardiac reserve that precedes systolic dysfunction in VEGF-B TG rats. (*A*) Representative H&E-stained cryosections display morphology of VEGF-B TG hearts showing cardiac hypertrophy at 3 weeks post DOCA-HS (left) and cardiac dilation at 6 weeks post DOCA-HS (right). Scale bar 100μm. Transthoracic echocardiography analyses of VEGF-B TG (circles) and WT (squares) ($n = 8$ animals/group; ***$P < 0.001$, **$P < 0.01$, *$P < 0.05$ vs. WT, ###$P < 0.001$, ##$P < 0.01$, #$P < 0.05$ vs. DOCA3w; two-way ANOVA *t*-test, Šidák post hoc). Structural and functional changes were evaluated dependent on time of DOCA + HS exposure (3 and 6 weeks DOCA-HS). (*B*) Left ventricular mass (LVMass) (*C*) end-diastolic diameters (LVESD) (*D*) relative wall thickness (RWTh) were validated with quantification of systolic parameters (*E*) FS, (*F*) EF, (*G*) stroke volume (SV), and (*H*) cardiac output (CO). (*I*) Pulse-wave Doppler at the mitral level of E (early filling) and A (atrial filling) ratio (E/A) and (*J*) E-wave with tissue Doppler e-wave ratio (E/e). Native cardiac and chronotropic reserve (stress-rest) in VEGF-B TG and WT rats were assessed with bolus dobutamine (1 mg/kg bw, i.p.) at baseline and 3 weeks of DOCA-HS. (*K*) Systolic performance expressed as delta LVESD mm (ΔLVESD) (*L*) chronotropic reserve expressed as delta heart rate (ΔHR) and (*M*, *N*) cardiac reserve delta FS and cardiac output (ΔFS, ΔCO, $n = 8$ animals/group; ***$P < 0.001$, *$P <$ 0.05 vs. WT, ###$P < 0.001$, #$P < 0.05$ vs. DOCA3w; two-way ANOVA *t*-test, Šidák post hoc). All data are depicted as dot plot with mean ± SE. Increased afterload universally led to diastolic dysfunction and cardiac fibrosis. Impaired inotropic and chronotropic reserve in VEGF-B TG predict systolic dysfunction in DOCA + HS induced dilated cardiomyocyte. VEGF-B TG rats thus recapitulate the structural and functional phenotype of many patients with HFrEF.

with a significant heart damage at Week 6 as shown by the elevated serum troponin (*Figure 3B*), which is a prognostic biomarker of myocardial injury in patients with cardiomyopathy.[23] At 6 weeks, the TG rats exhibited a decrease of both systolic and diastolic function, with a pronounced increase in the E/A ratio (*Figure 3A, C, D, and F*), and with accumulation of water in the heart and lungs (see Supplementary material online,

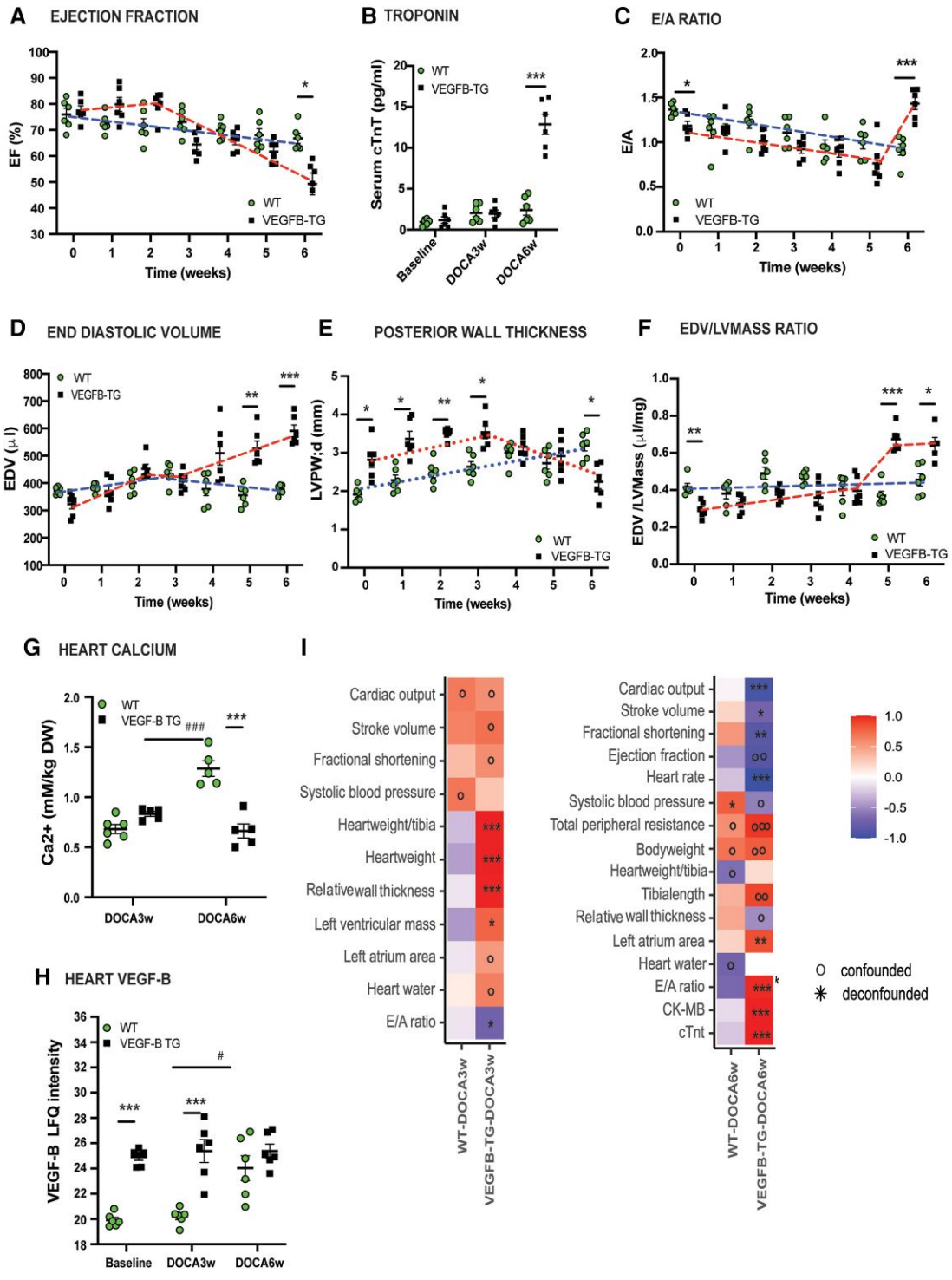

Figure 3 Longitudinal echocardiography of the transition to heart failure. The direction of heart function was negative with the progressing DOCA + HS. Dotted blue line, the direction in WT; dotted red line, the DOCA direction in VEGF-B TG. (*A*) Systolic parameter EF trajectory over time. All data are depicted as dot plots with mean ± SE, $n = 6$ analyzed by two-way repeated measures ANOVA with Tukey's post hoc test (genotype and time interactions). (*B*) Plasma Troponin, cardiac damage biomarker. Significance was assessed by unpaired, two-tailed *t*-test. (*C*) Diastolic parameter E/A trajectory over time $n = 6$. (*D*) LVPW; d (posterior wall thickness in diastole) trajectory over time. Heart geometric analysis of (*E*) end diastolic volume (EDV) and (*F*) EDV/LVMass ratio with an abrupt increase in TG at 5–6 weeks post DOCA + HS, dilatory phase. Significance was analyzed by two-way repeated measures ANOVA with Tukey's post hoc test. (*G*) Calcium concentration (Ca^{2+} mM/kg dry weight) and (*H*) VEGF-B protein levels (LFQ intensity) in WT and TG hearts. ***$P < 0.001$, vs. WT, ###$P < 0.001$, #$P < 0.05$ vs. DOCA3w; two-way ANOVA *t*-test, Šidák post hoc). (*I*) MetadeconfoundR output: impact of genotype (WT vs. TG) on clinical features, left 3 week DOCA- and right 6 week DOCA-treatment. Heatmap shows all clinical features with significant differences as per *Figure 1L*. LV remodelling and progressive dysfunction with DOCA + HS challenge is a longitudinal process that culminate into an end-stage heart failure in TG rats.

Figure S3C and D), suggestive of a restrictive filling pattern, which indicated a progressively worse diastolic dysfunction as the LV becomes increasingly abnormal (*Figure 3D*). Cardiac hypertrophy [left ventricle posterior wall thickness;d (LVPWd), *Figure 3E*] was associated with high calcium concentration (Ca^{2+}, *Figure 3G*) and VEGF-B protein expression (*Figure 3H*), whereas dilated TG hearts (EDV, *Figure 3D*) had suppressed cardiac Ca^{2+} levels (*Figure 3G*).

During the distinct cardiac dilation phase in the TG hearts from Week 4 to 6, the myocardial wall thickness was reduced (LVPW; d, 29%) in the VEGF-B TG rats (*Figure 3E*). However, the wall mass remained relatively constant, indicating that the endocardial surface increased relative to the epicardium (*Figure 2B*). Measures of cardiac volume and mass are typically represented as the ratio of cavity size and myocardial tissue mass (*Figure 3F*). The TG hearts demonstrated a brief, abruptly occurring (tipping-point) remodelling phase, during which this ratio increased by nearly 70% (*Figure 3F*). This transformation was clearly evident in the clustered univariate association heatmap of the phenotypic characteristics (*Figure 3I*), which had an unique effect size pattern for hypertrophic cardiomyopathy (HCM) (HW, RWTh) with LV diastolic dysfunction (E/A, LA area and heart water) at DOCA 3 week and DCM (RWTh) with LV systolic dysfunction (EF, SV, CO, and FS) at DOCA 6 week timepoint. The heatmap pattern (*Figure 3I*) also indicated that the cardiac damage markers troponin (c-Tnt) and creatinine kinase MB (CK-MB) are up-regulated only in the later phase of HF.

3.4 Diminished ATP plays a fundamental role in the failing VEGF-B TG hearts

We next asked whether the structural and functional remodelling in VEGF-B TG hearts is associated with metabolic adaptations or inotropic alterations, considering that a decreased heart energy status is an early pathomechanism in diastolic HF. Already at baseline, the TG rats demonstrated a doubling of their oxygen consumption (*Figure 4A*) and an approximately 30% increase in ATP relative to the WT rats (*Figure 4B*). The ATP level was dramatically increased in both TG and WT rats after 3 weeks of DOCA + HS, apparently because of an attempt to satisfy the higher energy requirements (*Figure 4B*). While cardiac ATP levels constantly increased during the treatment in synchrony with the increase in cardiac mass in the WT hearts, TG hearts started at a significantly higher ATP level at baseline, and showed a sudden drop in ATP at Week 6, leading to metabolic exhaustion concomitantly with the transition to systolic HF (*Figure 4B*).

3.5 Biphasic energy substrate response to mineralocorticoids

Metabolic flexibility is a remarkable virtue of the heart, which allows utilization of different energy substrates at different rates to maintain contractile function.[24] The failing heart shift its metabolism towards a greater reliance on glycolysis as a source of energy, which has been postulated to contribute to the reduced myocardial ATP level in the failing heart.[24] We evaluated the altered energy substrate utilization by applying a kinetic computational model of cardiac metabolism.[25] Changes in total heart substrate glucose, lactate, fatty acids (FAs), branched-chain amino acids (BCAA), ketone bodies, and ATP capacities were significant upon the DOCA-HS challenge (*Figure 4*; Supplementary material online, *Figure S4*). When comparing the total metabolic capacities, we found a biphasic trend of increased metabolic capacity from baseline to 3 weeks of DOCA-treatment and a regression at Week 6 in almost all substrates (*Figure 4C*; Supplementary material online, *Figure S4*). Both WT and TG rats demonstrated a clear increase in glycolytic capacity after 3 weeks DOCA + HS. This plateaued at 6 weeks in the WT rats, but deteriorated back to baseline in the TG rats (*Figure 4C*). Similarly, there was an increase in the FA utilization capacity at Week 3 and a regression after 6 weeks in both groups (*Figure 4D*). Importantly, the metabolic adaptation at Week 3 and the loss of metabolic capacity at Week 6 was much more pronounced in the TG than WT hearts. A similar trend was found for BCAA in the WT group and for lactate and ketone bodies in both groups (see Supplementary material online, *Figure S4B–D*). Noteworthy, there was a high variability between the individual rats within both groups, which likely reflects the idiosyncratic nature of the advanced progression of the disease. In particular, there was one outlier in the TG group at 3 weeks that had a non-hypertrophic phenotype with a slower rate of disease progression.

These changes in the maximal capacities for the substrate utilization for different energy delivering substrates were also reflected in the ATP concentrations of the hearts. *Figure 4E* shows the ATP capacities for each group. According to the model, at Week 3, the maximal heart ATP was significantly higher in the TG hearts than WT hearts, reflecting a higher metabolic compensation, possibly due to a higher demand as a response to the DOCA + HS treatment. During the transition to Week 6, heart ATP in both groups declined in the model, reaching a similar maximum ATP capacity, although the WT and TG hearts had diastolic HF and systolic HF phenotypes, respectively. Together with the directly measured ATP levels (*Figure 4B*), these data demonstrate that the failing TG hearts are not able to keep up with the ATP demand due to a decreased ATP capacity, e.g. through decreased creatin levels or spatial decoupling of ATP production and utilization. It is tempting to speculate, that Week 3 represents an early compensatory adaption of the metabolism, when the metabolic capacity increases to counterbalance the increased demand elicited by the DOCA + HS treatment. At Week 6, this adaptation vanishes, leaving the heart energetically challenged, but without the metabolic means to handle it, which in turn leads to a progressive HF. This interpretation is in line with the much higher compensation and subsequent loss of metabolic function in the TG hearts, which are seemingly much more susceptible to DOCA + HS treatment induced stress and suffer from a more severe HF after the prolonged DOCA + HS treatment. The distinct biphasic glucose and ATP profiles in the TG rats predict the onset of HF and contractile dysfunction.

3.6 Inotropic stimulation unravels metabolic abnormalities

Myocardial metabolic dysfunction may adversely influence the cardiac reserve under high-level pharmacological stress conditions. With intense cardiovascular activity (dobutamine-stress), the rate of ATP production and turnover goes up to sustain the cardiac reserve. At 3 weeks DOCA + HS, we demonstrated an increase in ATP capacity in TG hearts associated with compensatory hypertrophy. This increased energy capacity was evidently associated with impaired cardiac reserve (ΔEF, −5% and ΔFS, −10%, *Figure 4F and G*), which emphasizes energy exhaustion and metabolic abnormalities as general characteristics of reserve dysfunction in HFpEF.

3.7 Mitochondrial dysfunction precedes systolic dysfunction in VEGF-B-induced diastolic HF

Untargeted proteomics of the myocardial tissue comparing baseline, Week 3 and 6 was used to further explore which functional and biological pathways were significantly affected in the failing hearts. The detected proteins were mapped to higher level gene ontology (GO)-terms and categories using UniProt, while correcting for potential confounders (see Supplementary material online, *Methods*). Key metabolic and structural processes most likely involved in disease progression were picked up upon univariate testing among the different groups and time points (*Figures 5A and 6A*; Supplementary material online, *Figure S5*). Multiple metabolic pathways were significantly down-regulated in the TG rats at 3 weeks of DOCA+HS, including those related to mitochondrial processes (annotated under the terms cytochrome-c, ATPase2, and ATP channel activity), glycolysis (fumarylpyruvate, acetylpyruvate hydrolase, acylpyruvate hydrolase), amino acid metabolism (guanine metabolism), and purine metabolism (hypoxanthine). Repressed TCA cycle (pyruvate hydrolase activity) and mitochondrial ATP (hypoxanthin, guanine, and channel activity) were associated with impaired systolic function (CO, SV, and FS). Divergent findings were obtained in the treated WT rats. Predominately

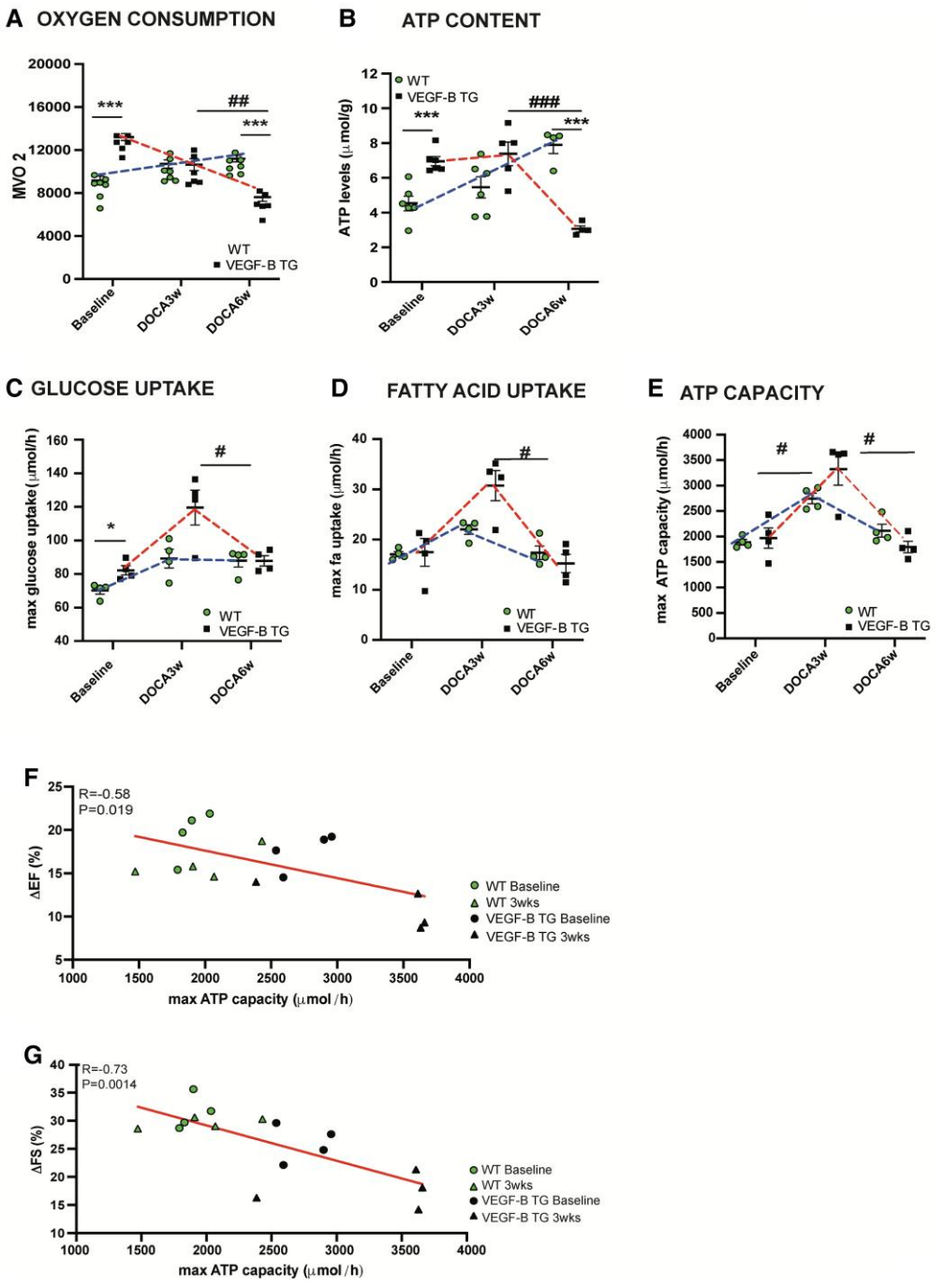

Figure 4 Enhanced energy consumption post DOCA + HS, predominately in VEGF-B TG rats leading to metabolic exhaustion and impaired cardiac reserve. (*A*) Oxygen consumption (µmol/min/g), (*B*) ATP concentration (µmol/g) in VEGF-B TG and WT rats prior and post 3 weeks DOCA + HS (DOCA3w) and 6 weeks DOCA + HS (DOCA6w) challenge. Whole heart metabolic substrate uptake of (*C*) glucose (*D*) FA and (*E*) ATP capacity, demonstrated biphasic response of increased energy consumption at DOCA3w and a regression at DOCA6w most striking in the TG rats ***$P < 0.001$, **$P < 0.01$, *$P < 0.05$ vs. WT; ##$P < 0.01$, #$P < 0.05$ vs. DOCA3w. Two-way ANOVA followed by Šidák post hoc test. VEGF-B TG rats demonstrate an inverse relationship between ATP capacity and cardiac systolic reserve of (*F*) ejection fraction (EF) and (*G*) FS post-dobutamine stress (Pearson's correlation, Student's *t*-test). In addition to heightened ATP levels TG rats also showed impairments in ATP energetics, which may have led to aggravate myocardial function during stress.

structural and cardiac stress related GO-terms were altered in analysis of the thus annotated proteins at 3 weeks (*Figure 6A*). To further illustrate this genotype-dependent metabolic switch, an inter-genotype comparison was done at 3 weeks of DOCA + HS treatment (see Supplementary material online, *Figure S5*). Shared metabolic GO terms were down-regulated in TG hearts and up-regulated in the WT hearts. These metabolic changes occurred already at 3 weeks of DOCA+HS in the preload-induced cardiomyopathy (see Supplementary material online, *Figure S5*). Accordingly,

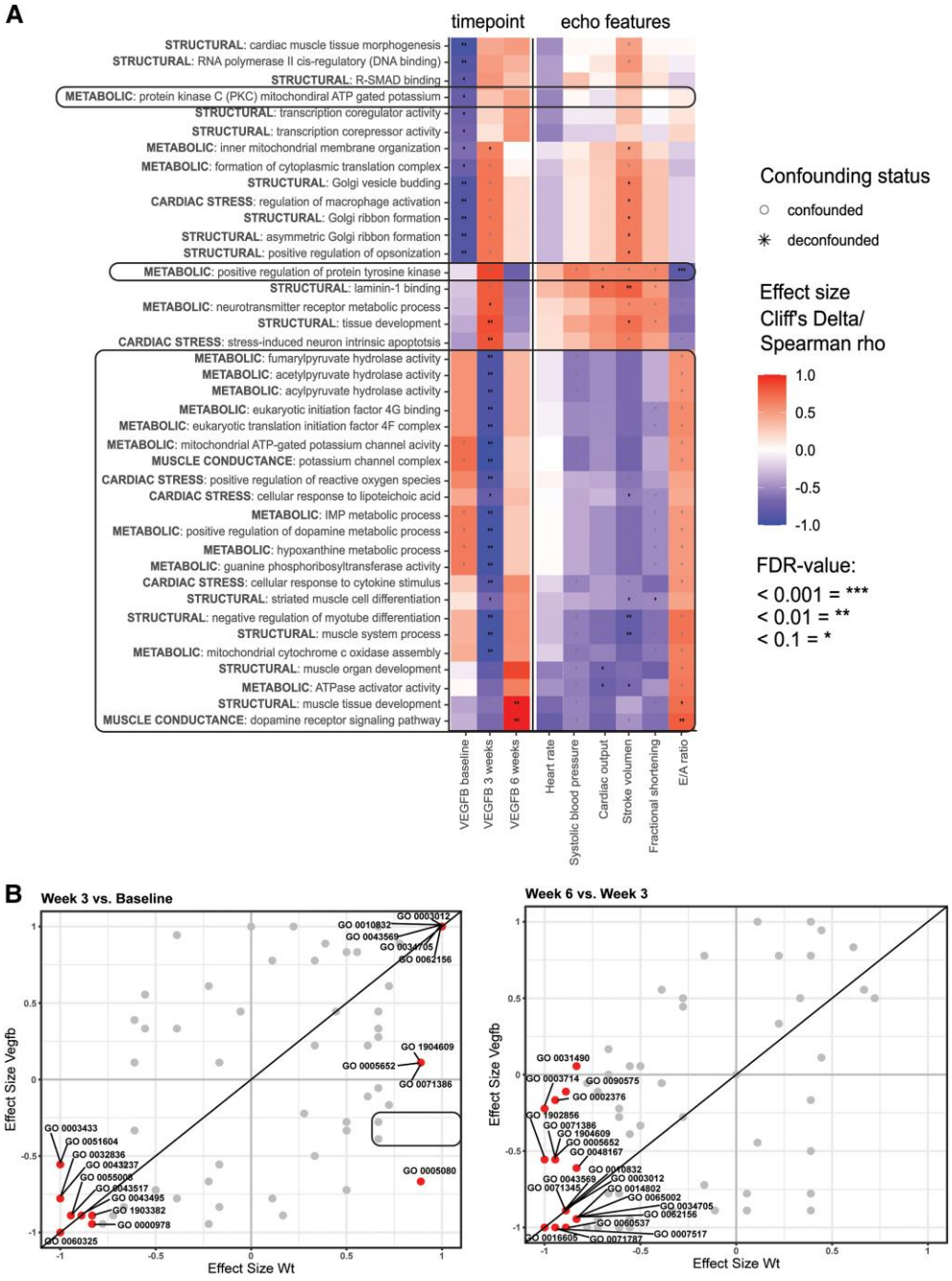

Figure 5 Metabolic intermediates of the TCA cycle were repressed in the VEGF-B TG hearts after DOCA + HS 3 weeks. (*A*) Time-series profiles of metabolic and structural protein (*x*-axis) in VEGF-B TG rats at baseline, Week 3 DOCA + HS and Week 6 DOCA + HS were correlated with echocardiographic parameters (*y*-axis), using Cliff's correlation FDR score blue represents positive correlations and red represents negative correlations. MetadeconfoundR analysis: impact of timepoint (VEGF-B only) and echo features on GO-terms different in differential Heatmap shows all clinical features with significant differences as per *Figure 1L*. (*B*) Differential effect of genotype and timepoint on detected proteins in the heart. Volcano plot showing changes in abundance (Cliff's delta effect size) of proteins binned by GO term annotations under intervention compared between genotypes (VEGF-B *y*-axis, wild-type *x*-axis). Left: 3 weeks DOCA treatment vs. baseline, right; 6 weeks vs. 3 weeks DOCA treatment. Labelled dots indicate those GO-terms for which this is significant (FDR-adjusted Wilcox test $Q < 0.1$) in both genotypes. GO-terms located on the vertical axis are similarly regulated in both genotypes, those located on the vertical axis exclusively regulated in VEGF-B and on the horizontal axis in wild-type hearts. GO:0005080 (PKC binding) was significantly opposed in regulation between TG and WT undergoing DOCA + HS intervention. Predominately metabolic adaptations in TG hearts after DOCA + HS challenge.

proteomic profiling was conducted to determine whether metabolic changes preceded the progression from compensated cardiac hypertrophy to HF. To identify GO terms that were differentially affected over time, we constructed volcano plots in which activities of genes binned to annotated GO terms were correlated with genotype (VEGF-B *y*-axis, WT *x*-axis, *Figure 5B*). We considered that changes in GO terms with time (Week 3

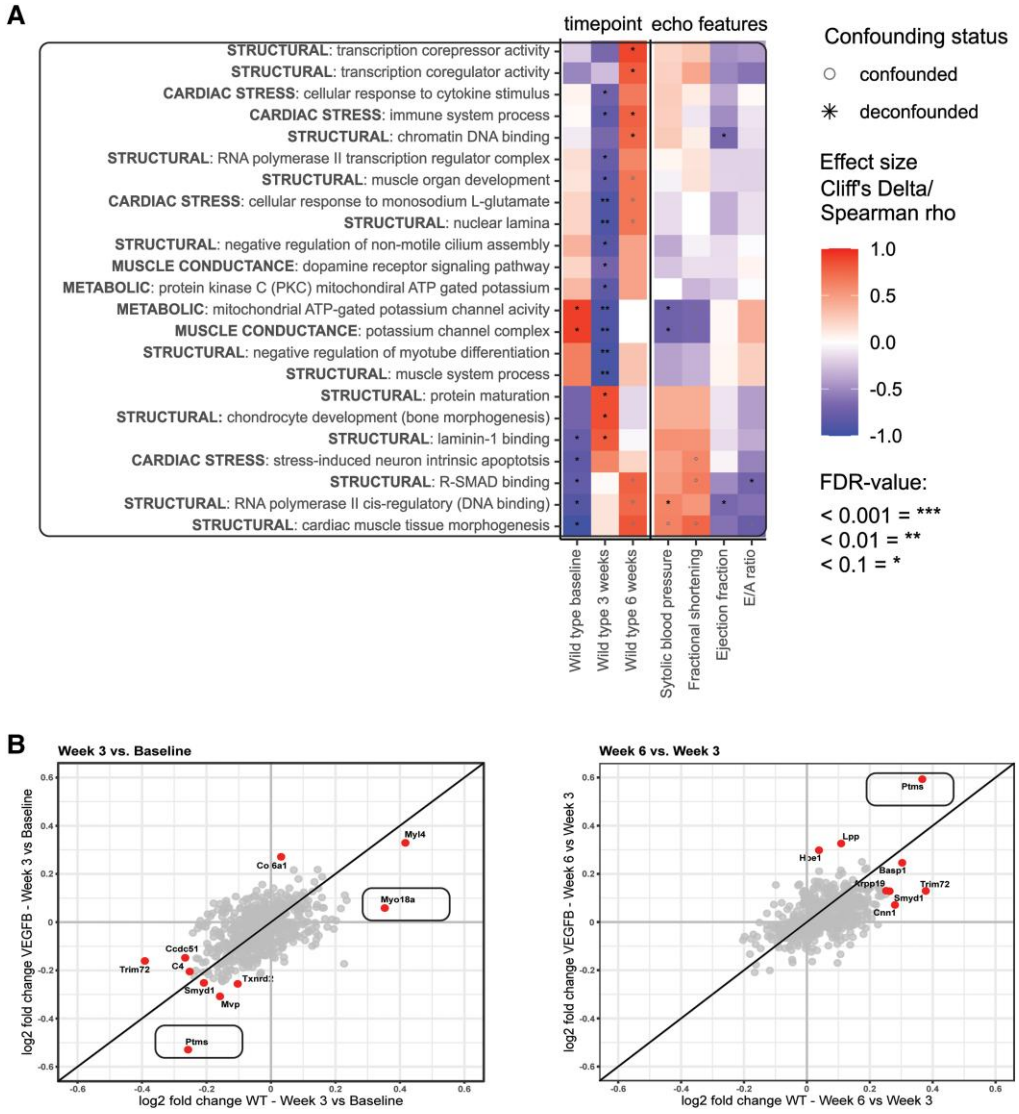

Figure 6 Structural and cardiac stress in WT and cardiac therapeutic targets in HF (*A*) MetadeconfoundR analysis of univariate biomarkers controlling for potential confounders: impact of time progression in WT rats and echocardiography features on abundance of proteins binned by GO term annotation significantly differential in abundance. Heatmap shows all clinical features with significant differences as per *Figure 1L*. (*B*) Effect of genotype and timepoint on fold changes (log2) of detected proteins in the heart. Labelled proteins indicate those proteins with an absolute log2-fold change higher than of 0.25 between the respective comparisons [left: wild-type 3 weeks vs. wild-type baseline ratio (*y*-axis) and VEGF-B 3 weeks vs. baseline ratio (horizontal axis), right: wild-type 6 weeks vs. wild-type 3 weeks ratio (vertical axis) and VEGF-B 6 weeks vs. 3 weeks ratio (horizontal axis)]. Proteins located on the vertical axis are similarly regulated in both genotypes, those located on the vertical axis exclusively regulated in VEGF-B and on the horizontal axis similarly solely in WT hearts. Predominately structural adaptations in WT hearts after DOCA + HS challenge.

vs. baseline and Week 6 vs. Week 3) may identify suitable therapeutic targets involved in the disease progression.

The opposite effect of protein kinase C (PKC) binding (GO:0005080), down-regulated in the TG hearts and up-regulated in the WT hearts in response to DOCA + HS treatment (*Figure 6B*), suggests that PKC is a mechanistic target in early HF progression. Another potential therapeutic target is lamininB1 (GO:1904609), which increased in WT hearts, but was unaltered in the TG hearts. Laminin deficiency has been associated with contractility defects and ATP deficiency in both DCM and HCM.[26] Epigenetic modification has been shown in HF progression and chromatin remodelling can be induced by cardiac stress and promote reactivation of foetal genes in the failing heart. Chromatin DNA binding (GO:0031490) was down-regulated in the WT rats but not in the TG rats after prolonged DOCA + HS treatment (6 weeks vs. 3 weeks). Targeting chromatin regulation may provide a promising approach to prevent and possibly reverse the myopathic process.[27]

In the DOCA + HS treated WT rats, the heatmap of GO biological activities revealed mainly structural and cardiac stress related processes (*Figure 6A*). Comparing GO biological processes, in the WT rats treated with DOCA + HS, there was an increase in fibrotic and hypertrophic growth processes at 3 weeks DOCA + HS (Laminin-1, R-SMAD, *Figure 6A*; Supplementary material online, *Figure S5*).

The volcano blots (with log2-fold change) identified few signatures that distinguished HFpEF from HFrEF, particularly in the metabolic pathways.

Ptms (parathymosin) changed with DOCA + HS challenge most prominently in the TG hearts (*Figure 6B*), being repressed at Week 3 and oppressed at Week 6 of DOCA + HS treatment, thus indicating HF

progression. Ptms has been identified in other HF models as an important diagnostic biomarker although its mechanism of action remains unknown. The other validated HF biomarkers Trim 72 (MG53) and Smyd1[28] were both switched with the progression of the disease, down-regulated at 3 weeks and up-regulated at 6 weeks in both genotypes (*Figure 6B*). A less responsive switch was obtained in the TG hearts, which is interesting as loss of Smyd1 function has been associated with the down-regulation of mitochondrial energetics prior to the onset of cardiac dysfunction.[28]

Finally, we compared our omics target data to a recently published clinical dataset[25] (Supplementary material online, *Method*). Ten cardiovascular-related proteins in our experimental study did overlap with clinical omics from patients with mitral valve insufficiency (MVI) and aortic stenosis (AS). Of these, two proteins (Gsk3b and Pdk4) are currently under evaluation in clinical trials for HF and eight (Ndufa1, Smad2, Col6a1, Serping1, Bcat, Hadhb, Psma6, and Tpm1) represent novel putative therapeutic targets for HF. Proteomics also identified invaluable disease-specific biomarkers for AS (Ndufa1, Bcat1, and Hadhb) and MVI (Gsk3b and Tpm1) (*Table 1*). The diverse changes in protein expression profiles between failing hearts induced by either AS or MVI demonstrated the heterogeneity of HF development. Understanding the differences in proteomic profiles could offer more precise therapeutic options for HF. Proteomic signatures (spectral counts) of Col6a1, Hadhb, and Smad2 were confirmed in the 3 and 6 weeks DOCA + HS VEGF-B TG with the expression in the AS and MVI patients (see Supplementary material online, *Figure S6*). GO analysis of the target proteins revealed enriched GO-terms associated with abundant acetylation, PI3K-Akt signalling pathway, and supramolecular fibre organization, Furthermore, Kyoto Encyclopedia of Genes and Genomes (KEGG) pathway analysis (see Supplementary material online, *Figure S7*) identified proteasomal and BCAA catabolism as hallmarks of failing hearts in both experimental (VEGF-B DOCA) as well as clinical HF (AS and MVI).

4. Discussion

In this study, we provide evidence that cardiac VEGF-B overexpression promotes the transition from diastolic HF to systolic HF in hypertensive rats with decreased functional cardiac reserve, accompanied by impaired substrate oxidation and ATP capacities. Already at baseline, mild signs of diastolic dysfunction without changes in the LV EF could be detected in the TG hearts. After increasing cardiac afterload upon treatment with an excess of mineralocorticoid and salt, the TG hearts showed an accelerated remodelling process leading from diastolic to systolic HF. Of note, the VEGF-B-mediated decline in cardiac function was associated with defective ATP bioenergetics. The early changes in cardiac energy homeostasis caused by VEGF-B preceded the systolic HF. Thus, alteration of cardiac metabolism is not an epiphenomenon, but rather a cause of HF. VEGF-B may thus provoke cardiac structural remodelling and mitochondrial impairment in hypertensive heart diseases.

Several studies have indicated that VEGF-B increases coronary vasculature growth and preserves both metabolic and cardiac function after acute MI and in ischaemia-reperfusion injury.[9,29] VEGF-B gene therapies were used to delay the development of HF in mice subjected to transverse aortic constriction.[30] Furthermore, VEGF-B gene transfer to prevented LV diastolic dysfunction short-term angiotensin II-infused rats.[31] Of note, these findings were observed in short-term studies, whereas long-term data were not reported. In our study, only a 6 week but not 3-week DOCA + HS challenge led to terminal heart phenotype. Therefore, experimental cardiovascular studies ought to more often consider a longitudinal study design. Nevertheless, some studies also reported adverse outcomes from chronic high-dose VEGF-B treatment, including impaired cardiac contractility, and paradoxically, arrythmias and cardiac arrest during dobutamine-induced cardiac stress.[8,22] TG mice that constitutively expressed high levels of the human VEGF-B 167 isoform developed cardiac hypertrophy that proceeded to fibrosis, ceramide accumulation and mitochondrial damage, and ultimately pre-term death.[32]

A key feature of our study design was the non-invasive longitudinal echocardiographic phenotyping in a cardiac hypertrophy model that by itself does not progress to pathological hypertrophy. We followed the trajectory of cardiac function loss during 6 weeks instead of the usual 3 weeks to understand the HF progression. Increased preload caused by the DOCA + HS challenge increased the concentric hypertrophy in the TG hearts until Week 4, when it was halted, with the development of DCM instead. This involved the thinning of the walls of the left ventricle, attenuation of EF and FS, and finally a dramatic elevation of cardiac cTnT levels. Thus, impaired cardiac reserve and diastolic dysfunction preceded the HFrEF pathology when VEGF-B was overexpressed.

In addition, we were able to study cross-sectionally, the role of VEGF-B on cardiac proteome and function in comparison to WT. Using unbiased confounder-corrected proteomic and targeted quantitative metabolomic profiling with correction for potential confounders, we found that although VEGF-B improves the control of FA oxidation, many genes involved in downstream mitochondrial energy transduction and ATP synthesis were significantly down-regulated in the DOCA + HS-treated TG hearts compared with baseline and WT hearts, respectively.

In striking contrast, myocardial proteome profiles were distinct in the different cardiac phenotypes, providing robust biomarkers for the transition to HF as well as distinguishing between pathological and physiological forms of cardiac hypertrophy. We found that a substantial proportion of metabolic proteins were down-regulated in the VEGF-B TG hearts, with the most dramatic effects at 3 weeks of DOCA + HS treatment, suggesting that the metabolic proteome changes precede the structural changes. Among these proteins were sub-units of pyruvate hydroxylase, the central enzyme enabling the transfer of carbons from glucose, pyruvate, and lactate into the TCA cycle and ATP citrate synthase. Pathways enriched in down-regulated enzymes were mitochondrial respiration (cytochrome c), purine metabolism (hypoxanthine), pentose phosphate pathway, and urea synthesis (guanine metabolism). Remarkably, the metabolites mentioned above, affected in the TG DOCA + HS-challenged hearts, were akin to protein changes in myocardial ischaemia as evidenced by amino acid depletion, glutathione depletion, increased oxidative stress, and evidence of aerobic energy production, thus suggesting impaired metabolic flexibility and furthermore an energy deficient state that further aggravates heart dysfunction.[33] At baseline, ATP levels in VEGF-B TG hearts were positively correlated with enhanced cardiac contractility, although we also observed first evidence of diastolic dysfunction. After the DOCA + HS challenge, the putative high ATP demand of VEGF-B TG rats could not be maintained, resulting in a long-term ATP deficit. The inefficient production of ATP in the TG hearts suggests that impaired mitochondrial OXPHOS is an early event of HF development.

The changes in the metabolic pathways were associated with inability to maintain normal contractility during stress (reduced inotropic reserve). Thus, our data reveal that VEGF-B predisposes the heart to dysfunction and damage during stress-induced metabolic demand. Previous studies have demonstrated that the regulation of VEGF-B in metabolism is mainly through its transcriptional control by PGC-1a, a key regulator of mitochondrial energetics.[34] The co-regulation of VEGF-B and mitochondrial proteins introduces a novel regulatory mechanism to explain how VEGF-B functions in the presence of DOCA + HS, when it switches to promotion of pathological mitochondrial energy metabolism.[32] Some proteins revealed an HF signature predicting the trajectory from a healthy to a diseased state. The mitochondrial ß-oxidation enzyme Hadhb shifted expression in the relation to the altered mitochondrial function in the VEGF-B TG rats. At baseline, VEGF-B TG rats demonstrated an up-regulation of Hadhb in correlation with the hypertrophy and later, loss of Hadhb with a significant decrease of mitochondrial energetics and DCM. Hadhb deficiency could potentially be an initial insult in the metabolic aggravation in HF. Hadhb mutations have been identified in MVI patients as well as in children with severe cardiomyopathy.[35,36]

Both TG and WT hearts demonstrated decreased abundance of proteins related to structural remodelling and contractile function. Changes in the microtubule cytoskeleton have been observed in the transition from

Table 1 HF proteomic profiling from animal model to human disease

Gene name	Fasta headers	WT DOCA	VEGF-B TG DOCA	AS	MVI
Bcat1	Branched-chain amino acid transaminase 1, cytosolic	Down (0.011)	Down (0.0063)	Down (1.3e−11)	ns
Pdk4	Pyruvate dehydrogenase kinase, isozyme 4	ns	Down (0.043)	Down (5.2e−5)	Down (0.0084)
Ndufa1	NADH dehydrogenase (ubiquinone) 1 alpha sub-complex, 1	ns	Down (0.023)	Down (0.037)	ns
Hadhb	Hydroxyacyl-CoA dehydrogenase/3-ketoacyl-CoA thiolase/enoyl-CoA hydratase, beta sub-unit	Down (0.021)	Down (0.0052)	Down (4.0e−6)	ns
Gsk3b	Glycogen synthase kinase 3 beta	ns	Up (5.9e−4)	ns	Up (0.039)
Psma6	Proteasome (prosome, macropain) sub-unit, alpha type 6	ns	ns	Up (0.026)	Up (0.0081)
Serping1	Serpin peptidase inhibitor, clade G (C1 inhibitor), member 1	ns	Up (0.0020)	Up (1.2e−3)	Up (2.9e−4)
Smad2	SMAD family member 2	Up (0.012)	Up (0.041)	Up (0.034)	Up (0.051)
Col6a1	Collagen, type VI, alpha 1	Up (6.7e−4)	Up (1.64e−5)	Up (3.8e−5)	Up (8.9e−6)
Tpm1	tropomyosin 1, alpha	ns	Up (0.0042)	ns	Up (0.030)

Gene name	Fasta headers	VEGF-B TG DOCA3	VEGF-B TG DOCA6	AS	MVI
Bcat1	Branched-chain amino acid transaminase 1, cytosolic	ns	Down (0.025)	Down (1.3e−11)	ns
Pdk4	Pyruvate dehydrogenase kinase, isozyme 4	Down (0.0011)	Down (0.0021)	Down (5.2e−5)	Down (0,0084)
Ndufa1	NADH dehydrogenase (ubiquinone) 1 alpha sub-complex, 1	Down (0.0019)	Down (1.0e−7)	Down (0.037)	ns
Hadhb	Hydroxyacyl-CoA dehydrogenase/3-ketoacyl-CoA thiolase/enoyl-CoA hydratase, beta sub-unit	Down (0.0023)	Down (3.2e−4)	Down (4.0e−6)	ns
Gsk3b	Glycogen synthase kinase 3 beta	ns	Up (5.9e−4)	ns	Up (0.039)
Psma6	Proteasome (prosome, macropain) sub-unit, alpha type 6	ns	Down (0.048)	Up (0.026)	Up (0.0081)
Serping1	Serpin peptidase inhibitor, clade G (C1 inhibitor), member 1	ns	Up (0.013)	Up (1.2e−3)	Up (2.9e−4)
Smad2	SMAD family member 2	Up (0.041)	Up (0.0012)	Up (0.034)	Up (0.051)
Col6a1	Tropomyosin 1, alpha	Up (0.0058)	Up (0.0047)	Up (3.8e−5)	Up (8.9e−6)
Tpm1	Branched-chain amino acid transaminase 1, cytosolic	ns	Up (0.0034)	ns	Up (0.030)

AS, aortic stenosis; MVI, mitral valve insufficiency, DOCA3, DOCA + high salt challenge 3 weeks; DOCA6, DOCA+ high salt-challenge 6 weeks.
Statistical changes compared with WT rats and healthy patients (one-way ANOVA, Tukey *t*-test for multiple comparisons, $n = 6–41$).

hypertrophy to HF,[37] where metabolic dysfunction may influence cardiac function and architecture of the cytoskeleton. There was also aberrant structural remodelling and fibrosis as the HF progressed. Collagen type I and VI expression were increased in the VEGF-B TG rats, influencing both contractile function and tension sensing.[38] Collagen VI sub-unit Col6a1, has been shown to stimulate fibroblast formation in infarcted heart tissue.[39] Proteomic analysis revealed enhanced Col6a1 protein expression in VEGF-B TG hearts that was also significantly increased in AS and MVI patients. Smad2 transcription was up-regulated in both VEGF-B TG and MVI hearts. Upon stress, TGFß/Smad2 signalling may participate increase the fibrotic gene programme in VEGF-B hearts[40] and it may provide an important biomarker in terms of clinical utility, i.e. prognosis, differential diagnosis, as well as disease progression and treatment monitoring. These pathways and their key-changing mediators need further validation in experimental models and clinical HF trials.

Our findings would corroborate data on impaired chronotropic and inotropic function after acute stress. TG rats showed a lower cardiac reserve in response to dobutamine stress, leading to functional damage in the long term. A higher abundance of intracellular Ca^{2+}-cycling proteins and the sarcoplasmic reticulum Ca^{2+} ATPase (ATP1a2) were observed in hypertrophic VEGF-B TG hearts at baseline, which was consistent with increased intracellular Ca^{2+} content. During the DOCA + HS hypertension, this was dramatically decreased in VEGF-B TG rats, suggesting that dysregulation of calcium transient homeostasis may contribute to the contractile dysfunction. The enhanced susceptibility to cardiac arrhythmias in the VEGF-B TG rats,[32] could be related to the impaired cardiac calcium homeostasis and energetics. Our data also indicated that mitochondrial ATP-gated potassium channel activity (K_{ATP}) was suppressed in TG hearts post DOCA + HS, which could lead to a failure of electrical responsiveness of cellular membranes and negative metabolic consequences. Approximately half of the overexpressed proteins were associated with muscle cardiomyopathy (tpm1, myl6), proteolytic degradation (rpn1, dad1), aging (serping1, gss), and stress response (hspa4, hyou1), suggesting enhanced energy demand (famine) and muscle weakness in the VEGF-B TG hearts.

4.1 Study limitations

Although we overexpressed VEGF-B in a cardiac-specific manner, the transgene resulted also in higher circulating VEGF-B186 levels. Therefore, our data need to be interpreted in light of direct cardiac VEGF-B actions plus possible peripheral actions on other organs, such as the kidney, which also showed a diminished function in the DOCA + HS treated VEGF-B TG rats. Furthermore, we did not use high-dose dobutamine to evaluate the biphasic response, in which contractile reserve occurs at low-dose and ischaemia at high-dose dobutamine, as we were concerned that high dose could provoke arrhythmias.[22] In fact, the dobutamine challenge protocol was stopped at Week 3, since two of the VEGF-B TG rats died of cardiac arrest. Another limitation of our study is that the small sample sizes in the sub-study (kinetic model of cardiac metabolism) preclude analysis of some substrate shifts in the pathogenesis of HF.

5. Conclusion

Our study offers mechanistic insights on VEGF-B promoted HF progression in hypertension, along with new insights on the role of cardiac metabolism in cardiac pathology. Our data utilizing longitudinal proteomics to reveal metabolic and structural remodelling in the transition to advanced HF highlight the slowly evolving nature of HCM. Our results further point to the important role of mitochondria, specifically ATP homeostasis, in HF. Myocardial ATP drastically drops in the context of clinically advanced HF (LV wall-thinning, troponin, and reduced EF). The proteomic analysis demonstrated

several 'danger' signals related to ATP deficiency, being VEGF-B overexpression. Finally, we identifed 10 target proteins in human cardiovascular disease, with mitral valve insufficiency (MVI) and aortic stenosis (AS), which integrated multi-omics datasets revealed concordant changes in protein profiles. Our study highlights an opportunity for human target prioritization enabled by proteomic analysis of animal models. Proteome-wide studies provide both direct associations with target outcomes (diastolic HF, systolic HF) and HF disease sub-types (MVI, AS), providing new tools for the discovery of therapeutic targets and their prioritization.

Supplementary material

Supplementary material is available at *Cardiovascular Research* online.

Authors' contributions

A.-M.S. led the project, designed and performed most experiments, analyzed and interpreted the data. T.U.P.B. and H.A. conducted the proteomic study, under the supervision of S.K.F. and performed confounded corrected statistical analysis together with L.M. K.F. and S.K. performed proteomic validation analyses and O.T. the electrolyte HPLC analyses. I.T., E.N., I.S., and J.H. assisted with echocardiography, and performed protein experiments, general histology and collagen measurements. N.B. together with J.E. analyzed the Cardiokin experiments and N.B., and T.K. conducted the human proteomic analysis. H.N. regenerated the transgenic rats and performed breeding and genotyping. E.B., and K.A., I.S., and H.N provided the rat model advise and major conceptual input. T.S. and T.V.K. assisted with the animal experiments and data analyses. H.W. conceived the project. H.W. and D.N.M. supervised the experiments and interpreted the data. A.-M.S., D.N.M., and H.W. wrote the manuscript with key editing by K.A., E.B., and S.K.F. and further input from all authors.

Acknowledgements

We thank Even Birkeland (PROBE UiB) and Kathrin Textoris-Taube and Michael Muelleder (Charite) for conducting protein analysis using mass spectrometry.

Conflict of interest: None declared.

Funding

A-M.S. and H.W. were supported by the Research Council of Norway (grant no. 262079), the Western Norway Regional Health Authority (nos F-12546 and 912168), and the Norwegian Health Association. D.N.M. and S.K.F. were supported by the Deutsche Forschungsgemeinschaft (DFG, German Research Foundation; Projektnummer 394046635-SFB 1365 and SFB1470 - A06 and A05, respectively); D.N.M. is supported by the Deutsches Zentrum für Herz-Kreislauf-Forschung (DZHK, 81Z0100106). K.A. is supported by the Wihuri Foundation, the Novo Nordisk Foundation, the Sigrid Jusélius Foundation and the Hospital District of Helsinki and Uusimaa. N.B., T.K and D.N.M. were supported by the Bundesministerium für Bildung und Forschung (German Federal Ministry of Education and Research), under the frame of ERA PerMed (HeartMed: grant 01KU2011A or 01KU2011B). N.B. was also funded by the DFG (SFB-1470 – A08 and project number 422215721).

Data availability

The data, analytical methods, and study materials that support the findings of this study are available from the corresponding authors on reasonable request.

References

1. Savarese G, Lund LH. Global public health burden of heart failure. *Card Fail Rev* 2017;**3**:7–11.
2. Nakamura M, Sadoshima J. Mechanisms of physiological and pathological cardiac hypertrophy. *Nat Rev Cardiol* 2018;**15**:387–407.
3. Bertero E, Sequeira V, Maack C. Hungry hearts. *Circ Heart Fail* 2018;**11**:e005642.
4. Chandler MP, Kerner J, Huang H, Vazquez E, Reszko A, Martini WZ, Hoppel CL, Imai M, Rastogi S, Sabbah HN, Stanley WC. Moderate severity heart failure does not involve a downregulation of myocardial fatty acid oxidation. *Am J Physiol Heart Circ Physiol* 2004;**287**:H1538–H1543.
5. Lopaschuk GD, Karwi QG, Tian R, Wende AR, Abel ED. Cardiac energy metabolism in heart failure. *Circ Res* 2021;**128**:1487–1513.
6. Aase K, von Euler G, Li X, Ponten A, Thoren P, Cao R, Cao Y, Olofsson B, Gebre-Medhin S, Pekny M, Alitalo K, Betsholtz C, Eriksson U. Vascular endothelial growth factor-B-deficient mice display an atrial conduction defect. *Circulation* 2001;**104**:358–364.
7. Rasanen M, Sultan I, Paech J, Hemanthakumar KA, Yu W, He L, Tang J, Sun Y, Hlushchuk R, Huan X, Armstrong E, Khoma OZ, Mervaala E, Djonov V, Betsholtz C, Zhou B, Kivela R, Alitalo K. VEGF-B promotes endocardium-derived coronary vessel development and cardiac regeneration. *Circulation* 2021;**143**:65–77.
8. Kivela R, Bry M, Robciuc MR, Rasanen M, Taavitsainen M, Silvola JM, Saraste A, Hulmi JJ, Anisimov A, Mayranpaa MI, Lindeman JH, Eklund L, Hellberg S, Hlushchuk R, Zhuang ZW, Simons M, Djonov V, Knuuti J, Mervaala E, Alitalo K. VEGF-B-induced vascular growth leads to metabolic reprogramming and ischemia resistance in the heart. *EMBO Mol Med* 2014;**6**:307–321.
9. Hagberg CE, Falkevall A, Wang X, Larsson E, Huusko J, Nilsson I, van Meeteren LA, Samen E, Lu L, Vanwildemeersch M, Klar J, Genove G, Pietras K, Stone-Elander S, Claesson-Welsh L, Ylä-Herttuala S, Lindahl P, Eriksson U. Vascular endothelial growth factor B controls endothelial fatty acid uptake. *Nature* 2010;**464**:917–921.
10. Ammarguellat F, Larouche I, Schiffrin EL. Myocardial fibrosis in DOCA-salt hypertensive rats: effect of endothelin ET(A) receptor antagonism. *Circulation* 2001;**103**:319–324.
11. Ardehali H, Sabbah HN, Burke MA, Sarma S, Liu PP, Cleland JG, Maggioni A, Fonarow GC, Abel ED, Campia U, Gheorghiade M. Targeting myocardial substrate metabolism in heart failure: potential for new therapies. *Eur J Heart Fail* 2012;**14**:120–129.
12. Zhou B, Tian R. Mitochondrial dysfunction in pathophysiology of heart failure. *J Clin Invest* 2018;**128**:3716–3726.
13. Devaux Y, Vausort M, Azuaje F, Vaillant M, Lair ML, Gayat E, Lassus J, Ng LL, Kelly D, Wagner DR, Squire IB. Low levels of vascular endothelial growth factor B predict left ventricular remodeling after acute myocardial infarction. *J Card Fail* 2012;**18**:330–337.
14. Wang L, Yu P, Zhou B, Song J, Li Z, Zhang M, Guo G, Wang Y, Chen X, Han L, Hu S. Single-cell reconstruction of the adult human heart during heart failure and recovery reveals the cellular landscape underlying cardiac function. *Nat Cell Biol* 2020;**22**:108–119.
15. Bry M, Kivela R, Holopainen T, Anisimov A, Tammela T, Soronen J, Silvola J, Saraste A, Jeltsch M, Korpisalo P, Carmeliet P, Lemstrom KB, Shibuya M, Yla-Herttuala S, Alhonen L, Mervaala E, Andersson LC, Knuuti J, Alitalo K. Vascular endothelial growth factor-B acts as a coronary growth factor in transgenic rats without inducing angiogenesis, vascular leak, or inflammation. *Circulation* 2010;**122**:1725–1733.
16. Robciuc MR, Kivelä R, Williams IM, de Boer JF, van Dijk TH, Elamaa H, Tigistu-Sahle F, Molotkov D, Leppänen VM, Käkelä R, Eklund L, Wasserman DH, Groen AK, Alitalo K. VEGFB/VEGFR1-induced expansion of adipose vasculature counteracts obesity and related metabolic complications. *Cell Metab* 2016;**23**:712–724.
17. Glezeva N, Voon V, Watson C, Horgan S, McDonald K, Ledwidge M, Baugh J. Exaggerated inflammation and monocytosis associate with diastolic dysfunction in heart failure with preserved ejection fraction: evidence of M2 macrophage activation in disease pathogenesis. *J Card Fail* 2015;**21**:167–177.
18. Kohlhaas M, Nickel AG, Maack C. Mitochondrial energetics and calcium coupling in the heart. *J Physiol* 2017;**595**:3753–3763.
19. Pimenta E, Gordon RD, Stowasser M. Salt, aldosterone and hypertension. *J Hum Hypertens* 2013;**27**:1–6.
20. Plante E, Lachance D, Drolet MC, Roussel E, Couet J, Arsenault M. Dobutamine stress echocardiography in healthy adult male rats. *Cardiovasc Ultrasound* 2005;**3**:34.
21. Marwick TH, Case C, Sawada S, Rimmerman C, Brenneman P, Kovacs R, Short L, Lauer M. Prediction of mortality using dobutamine echocardiography. *J Am Coll Cardiol* 2001;**37**:754–760.
22. Lahteenvuo J, Hatinen OP, Kuivanen A, Huusko J, Paananen J, Lahteenvuo M, Nurro J, Hedman M, Hartikainen J, Laham-Karam N, Makinen P, Rasanen M, Alitalo K, Rosenzweig A, Yla-Herttuala S. Susceptibility to cardiac arrhythmias and sympathetic nerve growth in VEGF-B overexpressing myocardium. *Mol Ther* 2020;**28**:1731–1740.
23. Kubo T, Ochi Y, Baba Y, Sugiura K, Takahashi A, Hirota T, Yamanaka S, Yamasaki N, Doi YL, Kitaoka H. Elevation of high-sensitivity cardiac troponin T and left ventricular remodelling in hypertrophic cardiomyopathy. *ESC Heart Fail* 2020;**7**:3593–3600.
24. Doenst T, Nguyen TD, Abel ED. Cardiac metabolism in heart failure: implications beyond ATP production. *Circ Res* 2013;**113**:709–724.
25. Berndt N, Eckstein J, Wallach I, Nordmeyer S, Kelm M, Kirchner M, Goubergrits L, Schafstedde M, Hennemuth A, Kraus M, Grune T, Mertins P, Kuehne T, Holzhütter HG. CARDIOKIN1: computational assessment of myocardial metabolic capability in healthy controls and patients with valve diseases. *Circulation* 2021;**144**:1926–1939.
26. Brayson D, Shanahan CM. Current insights into LMNA cardiomyopathies: existing models and missing LINCs. *Nucleus* 2017;**8**:17–33.
27. Liu CF, Tang WHW. Epigenetics in cardiac hypertrophy and heart failure. *JACC Basic Transl Sci* 2019;**4**:976–993.
28. Warren JS, Tracy CM, Miller MR, Makaju A, Szulik MW, Oka SI, Yuzyuk TN, Cox JE, Kumar A, Lozier BK, Wang L, Llana JG, Sabry AD, Cawley KM, Barton DW, Han YH, Boudina S, Fiehn O, Tucker HO, Zaitsev AV, Franklin S. Histone methyltransferase Smyd1 regulates mitochondrial energetics in the heart. *Proc Natl Acad Sci U S A* 2018;**115**:E7871–E7880.

29. Kivela R, Hemanthakumar KA, Vaparanta K, Robciuc M, Izumiya Y, Kidoya H, Takakura N, Peng X, Sawyer DB, Elenius K, Walsh K, Alitalo K. Endothelial cells regulate physiological cardiomyocyte growth via VEGFR2-mediated paracrine signaling. *Circulation* 2019;**139**:2570–2584.
30. Huusko J, Merentie M, Dijkstra MH, Ryhanen MM, Karvinen H, Rissanen TT, Vanwildemeersch M, Hedman M, Lipponen J, Heinonen SE, Eriksson U, Shibuya M, Yla-Herttuala S. The effects of VEGF-R1 and VEGF-R2 ligands on angiogenic responses and left ventricular function in mice. *Cardiovasc Res* 2010;**86**:122–130.
31. Serpi R, Tolonen AM, Huusko J, Rysa J, Tenhunen O, Yla-Herttuala S, Ruskoaho H. Vascular endothelial growth factor-B gene transfer prevents angiotensin II-induced diastolic dysfunction via proliferation and capillary dilatation in rats. *Cardiovasc Res* 2011;**89**:204–213.
32. Karpanen T, Bry M, Ollila HM, Seppanen-Laakso T, Liimatta E, Leskinen H, Kivela R, Helkamaa T, Merentie M, Jeltsch M, Paavonen K, Andersson LC, Mervaala E, Hassinen IE, Yla-Herttuala S, Oresic M, Alitalo K. Overexpression of vascular endothelial growth factor-B in mouse heart alters cardiac lipid metabolism and induces myocardial hypertrophy. *Circ Res* 2008;**103**:1018–1026.
33. Wang X, Wang D, Wu J, Yu X, Lv J, Kong J, Zhu G, Su R. Metabolic characterization of myocardial infarction using GC-MS-based tissue metabolomics. *Int Heart J* 2017;**58**:441–446.
34. Mehlem A, Palombo I, Wang X, Hagberg CE, Eriksson U, Falkevall A. PGC-1alpha coordinates mitochondrial respiratory capacity and muscular fatty acid uptake via regulation of VEGF-B. *Diabetes* 2016;**65**:861–873.
35. Ojala T, Nupponen I, Saloranta C, Sarkola T, Sekar P, Breilin A, Tyni T. Fetal left ventricular noncompaction cardiomyopathy and fatal outcome due to complete deficiency of mitochondrial trifunctional protein. *Eur J Pediatr* 2015;**174**:1689–1692.
36. Ørstavik K, Arntzen KA, Mathisen P, Backe PH, Tangeraas T, Rasmussen M, Kristensen E, Van Ghelue M, Jonsrud C, Bliksrud YT. Novel mutations in the HADHB gene causing a mild phenotype of mitochondrial trifunctional protein (MTP) deficiency. *JIMD Rep* 2022;**63**:193–198.
37. Jane-Lise S, Corda S, Chassagne C, Rappaport L. The extracellular matrix and the cytoskeleton in heart hypertrophy and failure. *Heart Fail Rev* 2000;**5**:239–250.
38. Bogomolovas J, Brohm K, Celutkiene J, Balciunaite G, Bironaite D, Bukelskiene V, Daunoravicus D, Witt CC, Fielitz J, Grabauskiene V, Labeit S. Induction of ankrd1 in dilated cardiomyopathy correlates with the heart failure progression. *Biomed Res Int* 2015;**2015**:273936.
39. Moon J, Zhou H, Zhang LS, Tan W, Liu Y, Zhang S, Morlock LK, Bao X, Palecek SP, Feng JQ, Williams NS, Amatruda JF, Olson EN, Bassel-Duby R, Lum L. Blockade to pathological remodeling of infarcted heart tissue using a porcupine antagonist. *Proc Natl Acad Sci U S A* 2017;**114**:1649–1654.
40. Khalil H, Kanisicak O, Prasad V, Correll RN, Fu X, Schips T, Vagnozzi RJ, Liu R, Huynh T, Lee SJ, Karch J, Molkentin JD. Fibroblast-specific TGF-β-Smad2/3 signaling underlies cardiac fibrosis. *J Clin Invest* 2017;**127**:3770–3783.

Translational perspective

This work identifies the adverse effects of VEGF-B in the progression of heart failure (HF) in a rat model of pressure-induced hypertrophy. Long-term overexpression of VEGF-B in rat hearts accelerates the transition from mild to severe HF by maladaptive metabolic processes. VEGF-B boosts ATP production to compensate for the high ATP demand of the hypertrophic heart. In 6 weeks of treatment, DOCA-salt-induced hypertrophy resulted in a drastic drop in ATP synthesizing pathways, leading to impaired contractility. These findings disclose novel metabolic regulatory pathways with omics HF targets validated in patients with mitral valve insufficiency and aortic stenosis. Modulation of cardiac ATP levels provides an attractive therapeutic target for the treatment of cardiac hypertrophy and HF.